9-2018

CAMBER IN PRETENSIONED BRIDGE I-GIRDER IMMEDIATELY AFTER PRESTRESS TRANSFER

Jen-kan Kent Hsiao
hsiao@engr.siu.edu

Alexander Y. Jiang
alexjiang@siu.edu

CAMBER IN PRETENSIONED BRIDGE I-GIRDER IMMEDIATELY AFTER PRESTRESS TRANSFER

J. Kent Hsiao[1*] and Alexander Y. Jiang[2]

[1,2] Southern Illinois University Carbondale, Dept. of Civil and Environmental Engineering, USA
e-mail: hsiao@engr.siu.edu, alexjiang@siu.edu

ABSTRACT: Deflection control is an important design criterion for the serviceability of pretensioned concrete bridges. Upward cambers due to prestressing forces can be utilized to offset downward deflections due to gravity loads in order to control cracks and/or to produce desired cambers. The traditional hand-calculated approach simplifies the computation of pretensioned concrete girders by: (1) assuming that the prestressing force acting at the midspan of a girder remains constant along the entire span of the girder, (2) neglecting the p-δ effect on the girder due to the axial compression force in the girder, and (3) using the gross concrete section of the girder to compute the moment of inertia of the girder. The purpose of this work is to investigate the accuracy of the hand-calculated approach for the computation of cambers due to prestressing forces. The type of prestressed concrete girder investigated in this work is a pretensioned I-girder with a combination of straight strands and harped strands. The major findings derived from this work are: (1) the variation (non-uniformity) among prestressing forces acting along the tendons has no significant effect on the deflection of the girder, (2) the traditional hand-calculated approach neglecting the P-δ effect may result in considerably smaller girder deflections, and (3) the traditional hand-calculated approach using the moment of inertia of the gross concrete section (neglecting the additional stiffness contributed by tendons) may result in considerably larger girder deflections.

KEYWORDS: Bridges; Deflection; Finite element method; Girders; Prestressed concrete.

1 INTRODUCTION

Serviceability of a bridge refers to the performance of the bridge in service. Some of the most frequently considered serviceability issues with regard to prestressed concrete bridge girders relate to short- and long-term cambers or deflections. This paper focuses on the behavior of short-term cambers.

A camber is defined as an upward deflection induced at a point of a member from its position before application of a prestressing force to its position after application of the prestressing force. In a simply supported prestressed girder, a prestressing force typically produces an upward camber (since the prestressing force is usually applied below the centroid of the section), while the self-weight produces a downward deflection. The final deflection, therefore, depends on the combined effects of the prestressing force and the self-weight. Upward cambers due to prestressing forces can be utilized to offset downward deflections due to gravity loads in order to control cracks and/or to produce desired cambers. Typically, the downward deflection due to the self-weight of a prestressed bridge girder cannot be controlled, while the camber of the girder due to a prestressing force can easily be adjusted by changing the profile of the tendon or the magnitude of the prestressing force.

2 CAMBER COMPUTATION USING THE HAND-CALCULATED EQUIVALENT LOAD METHOD

A pretensioned element is a prestressed element in which the tendons are tensioned prior to casting the concrete. As shown in *Fig. 1,* the combination of two typical tendon profiles, straight strands and harped strands, are commonly used for the construction of precast, pretensioned bridge I-girders [1,2,3].

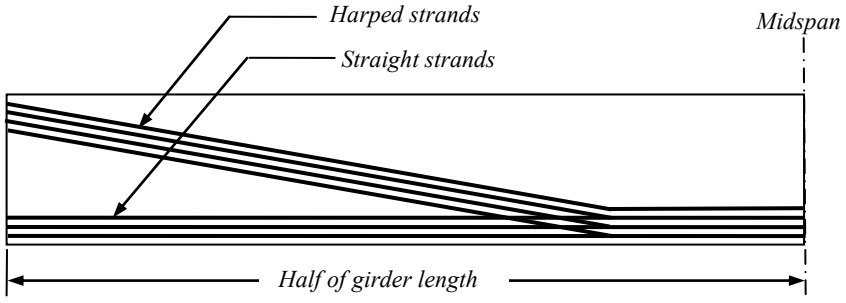

Figure 1. Longitudinal strand profile of a precast, pretensioned bridge I-girder

The equivalent load method treats the concrete girder as an elastic member loaded by the prestressed tendon reactions. According to this method, the tendon can be removed and the forces it exerts on the girder are treated as loads. The equivalent loads for straight tendons and harped tendons are shown in *Figs. 2(b)* and *3(b),* respectively [4, 5], while *Fig. 4* shows the deflections at the midspan of a simply supported beam due to various loading conditions [6]. Camber computation can be performed using the equivalent loads induced by the strand profiles shown in *Figs. 2 & 3* and the deflection computation formulas shown in *Fig. 4*.

Referring to *Figs. 2(b)* and *4(a)*, the midspan camber due to the prestressing force for the simply supported beams shown in *Fig. 2(a)* can be computed using Eq. (1):

$$\Delta = \frac{L^2}{8EI}\left(P_s \cdot e\right) \tag{1}$$

where: Δ is the midspan camber,
L is the span length,
P_s is the prestressing force,
e is the eccentricity between the center of gravity of the tendon area and the center of gravity of the concrete section,
E is the modulus of elasticity of concrete, and
I is the moment of inertia of the section resisting externally applied loads.

Also, referring to *Figs. 3(b), 4(a),* and *4(b)*, the midspan camber due to the prestressing force for the simply supported beams shown in *Fig. 3(a)* can be computed using Eq. (2):

$$\Delta = \frac{P_s(e_1)}{24EI}(3L^2 - 4a^2) + \frac{L^2}{8EI}(P_s \cdot e_2) \tag{2}$$

where: e_1 is the sag at the mid-span of the depressed tendon, and
e_2 is the vertical distance between c.g.s. (center of gravity of prestressed steel) and c.g.c. (center of gravity of concrete section) at the end section.

Note that the following assumptions have been made for the development of the Eqs. (1) & (2):

a) The prestressed concrete is a homogeneous elastic body which closely obeys the ordinary laws of flexure and shear.
b) Deflections due to shear deformation are small and therefore may be disregarded.
c) The uncracked concrete cross-sectional area is used to compute the moment of inertia. Therefore, if the computed tensile stress in concrete immediately after prestress transfer exceeds $6\sqrt{f'_{ci}}$ (where f'_{ci} is the compressive strength of concrete at time of initial prestress) at the ends of simply supported members, or $3\sqrt{f'_{ci}}$ at other locations, additional bonded reinforcement shall be provided in the tensile zone to resist the total tensile force in concrete computed with the assumption of an uncracked section [7].

d) The magnitude of the prestressing force acting on the girder remains unchanged throughout the entire span of the girder.

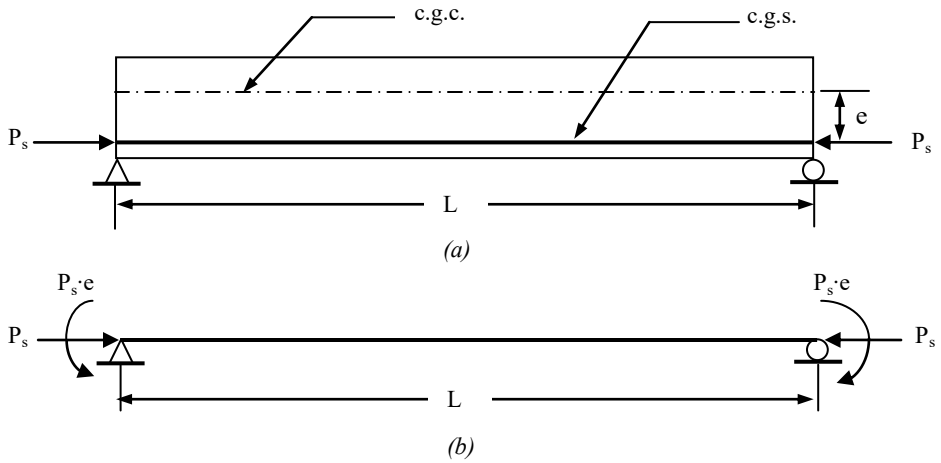

Figure 2. Equivalent loads for straight tendons

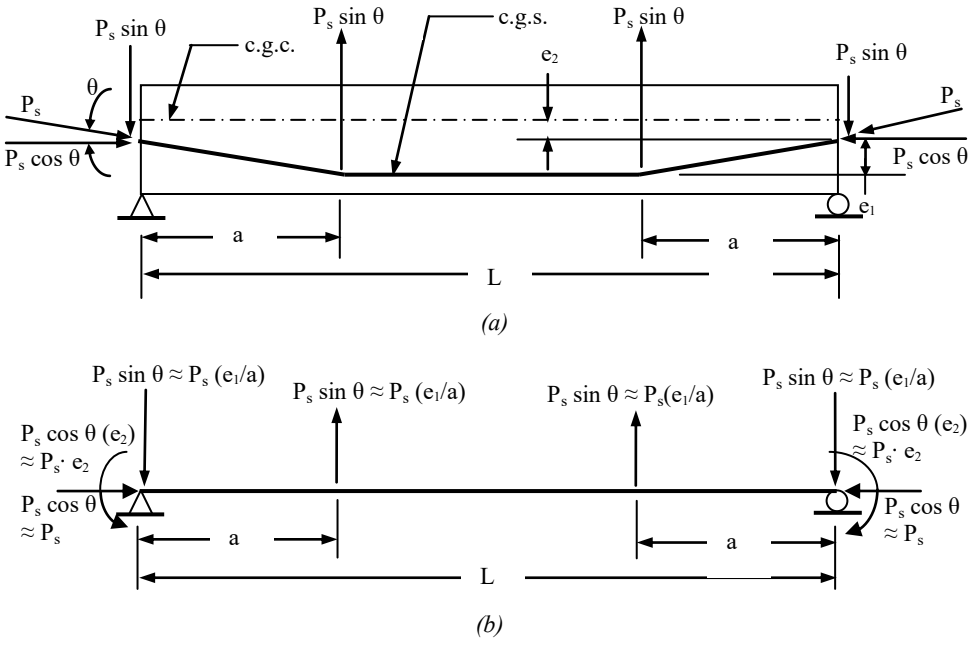

Figure 3. Equivalent loads for harped tendons

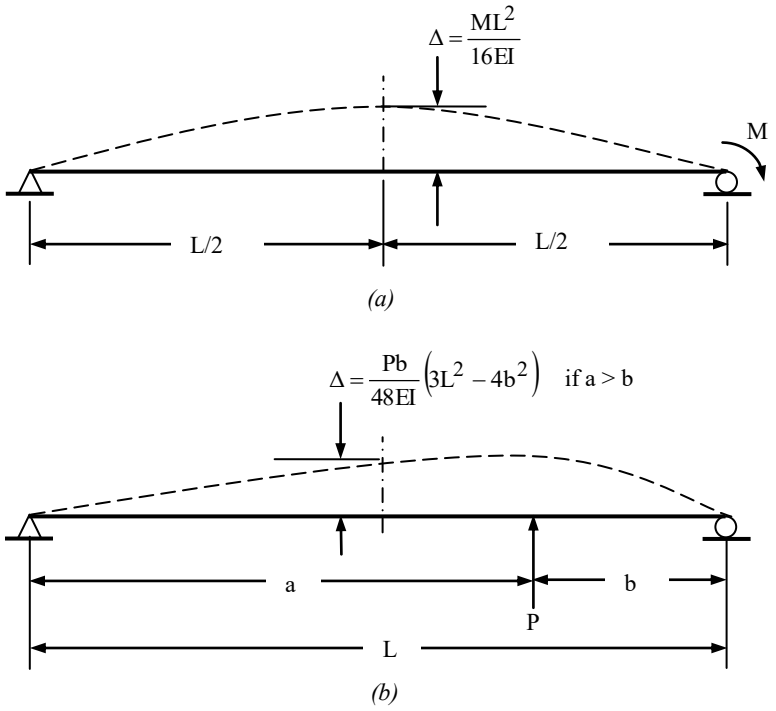

Figure 4. Beam deflections at midspan due to various loading conditions

3 LOSS OF PRESTRESS DUE TO THE ELASTIC SHORTENING IN PRETENSIONED GIRDERS

Immediately after the prestressing force is transferred to a pretensioned concrete girder, the girder shortens and the prestressed tendons shorten with it, resulting in the loss of prestress in the tendons.

Prestress loss due to the elastic shortening in pretensioned girders can be computed using Eq. (3):

$$\Delta f_{pES} = \frac{E_p}{E_{ci}} f_{cgp} \tag{3}$$

where: E_p is the modulus of elasticity of prestressed steel,
E_{ci} is the modulus of elasticity of concrete at time of initial prestress, and
f_{cgp} is the stress in concrete at the center of gravity of prestressed steel immediately after the prestressing force has been applied to the concrete, that is:

$$f_{cgp} = -\frac{P_i}{A_g} - \frac{(P_i e_m) e_m}{I_g} + \frac{M_g e_m}{I_g} \quad (4)$$

where: A_g is the gross area of the girder section,
e_m is the average prestressed steel eccentricity at the midspan of the girder,
I_g is the moment of inertia of the gross concrete section,
M_g is the moment at the midspan due to the self-weight of the girder, and
P_i is the prestressing force in tendons immediately after prestress loss due to the elastic shortening of concrete, that is:

$$P_i = A_{ps}\left(f_{pbt} - \Delta f_{pES}\right) \quad (5)$$

where: A_{ps} is the area of prestressed steel, and
f_{pbt} is the stress in prestressed steel immediately prior to prestress transfer.

The prestressing force in tendons immediately after prestress loss due to the elastic shortening of concrete may be assumed to be 90 percent of the initial prestressing force before prestress transfer and the analysis iterated until an acceptable accuracy is achieved. Alternatively, to avoid iteration, Δf_{pES} can be computed using Eq. (6) [8]:

$$\Delta f_{pES} = \frac{A_{ps} f_{pbt} (I_g + e_m^2 A_g) - e_m M_g A_g}{A_{ps}(I_g + e_m^2 A_g) + \frac{A_g I_g E_{ci}}{E_p}} \quad (6)$$

4 PRESTRESSING FORCE SIMULATION

The theory of "thermal effects on steel" is utilized in this paper to simulate prestressing forces in tendons. The change in unit stress in prestressed steel due to the change in temperature of the steel can be computed using Eq. (7)[9]:

$$\text{Change in unit stress} = E_p \varepsilon (\Delta t) \quad (7)$$

where: E_p is the modulus of elasticity of prestressed steel,
ε is the thermal expansion coefficient of prestressed steel, and
Δt is the change in temperature of prestressed steel.

The computed stresses in Eq. (7) in turn can be utilized to simulate the prestressing force in prestressed steel using Eq. (8):

$$\text{Simulated prestressing force} = A_{ps}E_p\varepsilon(\Delta t) \quad (8)$$

where: A_{ps} is the area of prestressed steel.

Since the change in unit stress in prestressed steel is the product of "ε" and "Δt ," any expected prestressing force can be simulated by using a random value of "ε" multiplied by a corresponding "Δt" value.

5 CAMBER COMPUTATION EXAMPLE

The example demonstrated below is for the computation of the camber for a pretensioned concrete girder due to prestressing forces immediately after prestress transfer.

A concrete girder with a 96-ft simple span, as shown in *Fig. 5,* is pretensioned using 40-0.5 in. diameter low-relaxation strands ($A_{ps} = 40 \times 0.153$ in.$^2 = 6.12$ in.^{2}) with a modulus of elasticity (E_p) of 28,500 ksi. Compute the camber at midspan due to a prestressing force immediately after prestress transfer assuming that: (1) f_{pu} (specified tensile strength of prestressed steel) = 270 ksi, (2) f_{pbt} (the stress in prestressed steel immediately prior to prestress transfer) = $0.75f_{pu}$, and (3) E_{ci} (the modulus of elasticity of concrete at time of initial prestress) = 4458 ksi.

5.1 Compute the moment of inertia of the gross concrete section

Computation of the moment of inertia about the centroidal axis of the uncracked gross concrete section of the girder shown in *Fig. 6* is shown in Table 1.

Table 1. Computation of the moment of inertia of the gross concrete section

segment	area (in.^{2})	Y (in.)[a]	Ay (in.^{3})	Ay^2 (in.^{4})	I_o (in.^{4})[b]
(1)	112	1.75	196	343	114
(2)	55	2.75	151.25	416	139
(3)	32	4.167	133.33	556	7
(4)	4	6.167	24.67	152	1
(5)	291	29.75	8,657.25	257,553	57,042
(6)	45	46.5	2,092.5	97,301	51
(7)	120	51	6,120	312,120	360
Σ	659		17,375	668,441	57,714

[a] y = the distance from the centroid of a segment to the top fiber of the gross concrete section.

[b] I_o = the moment of inertia of a segment about its centroidal axis.

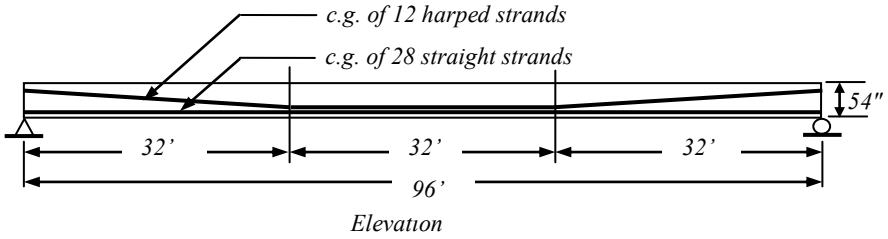

Elevation

No. of Strands	Distance from conc. bottom fiber
12	2"
12	4"
8	6"
4	8"
2	10"
2	12"

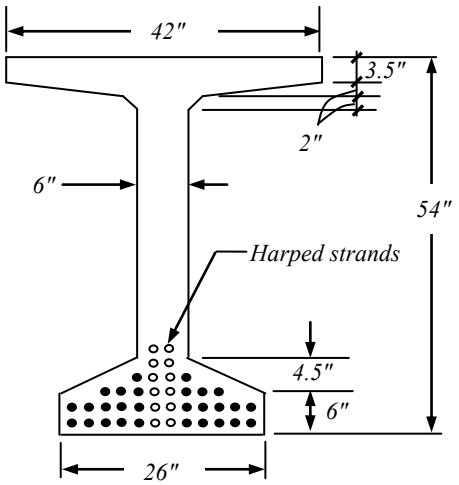

Cross section at harp points and midspan

No. of Strands	Distance from conc. bottom fiber
10	2"
10	4"
6	6"
2	8"
2	42"
2	44"
2	46"
2	48"
2	50"
2	52"

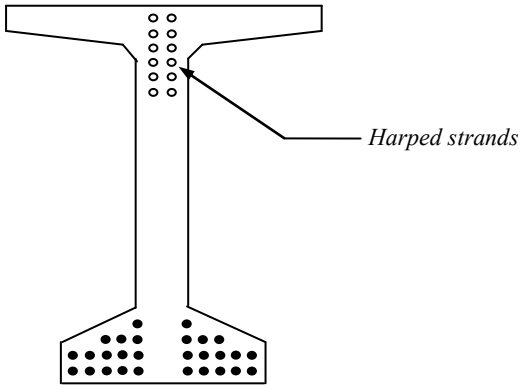

Cross section at ends

Figure 5. The elevation and cross sections of the Pretensioned concrete girder example

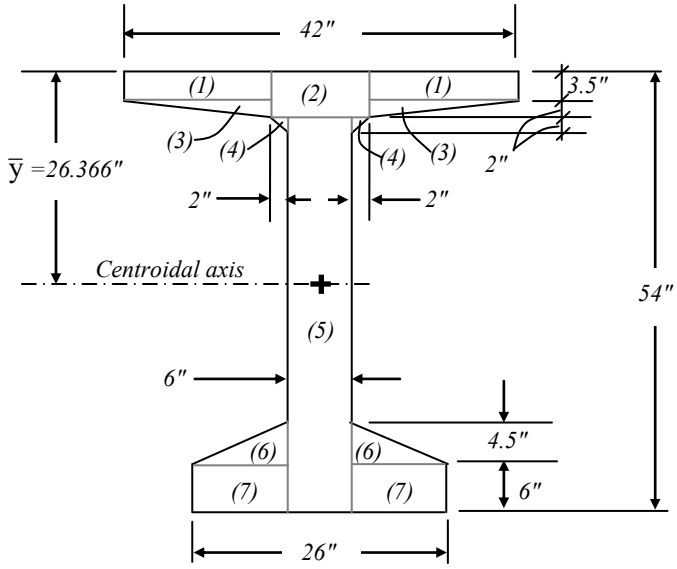

Figure 6. Gross section of the I-girder for the camber computation example

From Table 1, the distance from the centroidal axis of the gross section to the extreme top fiber of the section can be computed to be:

$$\bar{y} = \frac{\Sigma Ay}{\Sigma A} = \frac{17{,}375}{659} = 26.3657 \text{ in.}$$

The location of the centroidal axis of the gross section of the girder is shown in *Fig. 6*. Furthermore, the moment of inertia of the gross section about the centroidal axis of the section can be computed to be:

$$\begin{aligned} I &= \sum I_o + \sum Ay^2 - \sum A(\bar{y})^2 \\ &= 57{,}714 + 668{,}441 - 659(26.3657)^2 \\ &= 268{,}051 \text{ in.}^4 \end{aligned}$$

5.2 Locate the center of gravity of the prestresssing steel in the girder

Referring to Fig. 5, the distance between the centroid of the 28 straight strands and the extreme bottom fiber of the girder at all locations is:

$$\frac{10(2'') + 10(4'') + 6(6'') + 2(8'')}{10 + 10 + 6 + 2} = 4 \text{ in.}$$

The distance between the centroid of the 12 harped strands and the extreme bottom fiber of the girder at the girder ends is:

$$\frac{2(42'' + 44'' + 46'' + 48'' + 50'' + 52'')}{2(6)} = 47 \text{ in.}$$

The distance between the centroid of the 12 harped strands and the extreme bottom fiber of the girder at the harp points and the midspan is:

$$\frac{2(2'' + 4'' + 6'' + 8'' + 10'' + 12'')}{2(6)} = 7 \text{ in.}$$

The longitudinal strand profile and the locations of the centroids of the harped and straight strands at the ends, the harp points, and the midspan of the girder are shown in *Fig. 7*.

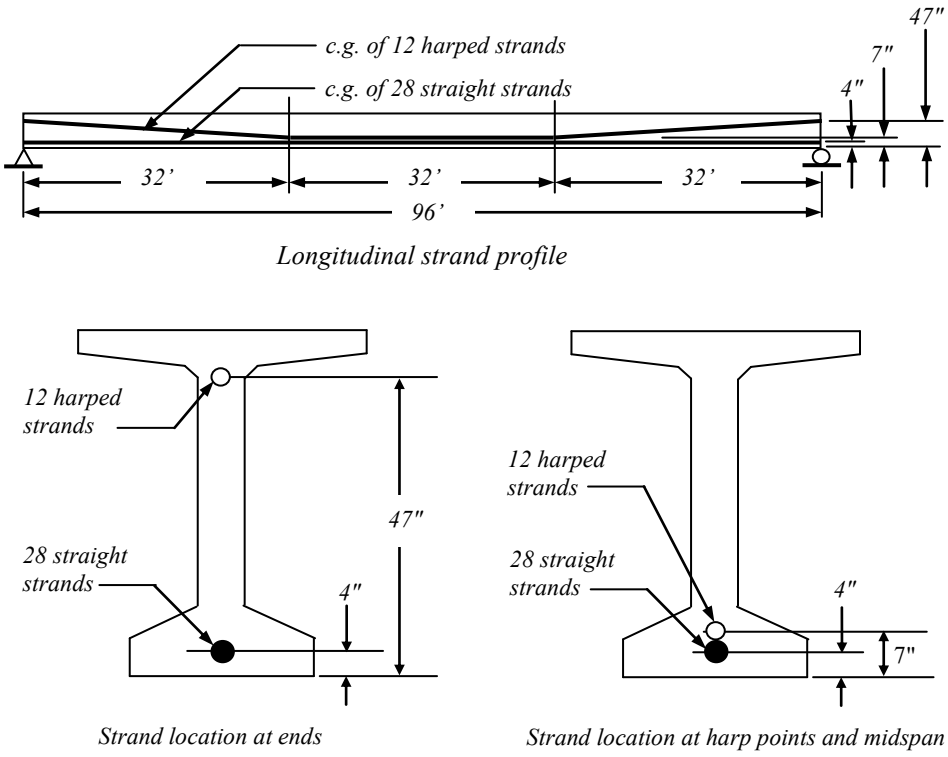

Figure 7. Longitudinal strand profile and locations of centroids of straight and harped strands

Also, referring to *Fig. 5*, the distance between the centroid of the 40 combined straight and harped strands and the extreme bottom fiber of the girder at the harp points and the midspan is:

$$\frac{12(2'') + 12(4'') + 8(6'') + 4(8'') + 2(10'') + 2(12'')}{12 + 12 + 8 + 4 + 2 + 2} = 4.9 \text{ in.}$$

The distance between the centroid of the 40 combined straight and harped strands and the extreme bottom fiber of the girder at the girder end is:

$$\frac{10(2'') + 10(4'') + 6(6'') + 2(8'' + 42'' + 44'' + 46'' + 48'' + 50'' + 52'')}{40} = 16.9 \text{ in.}$$

The longitudinal strand profile and the locations of the centroid of the combined straight and harped strands at the ends, the harp points, and the midspan are shown in *Fig. 8.*

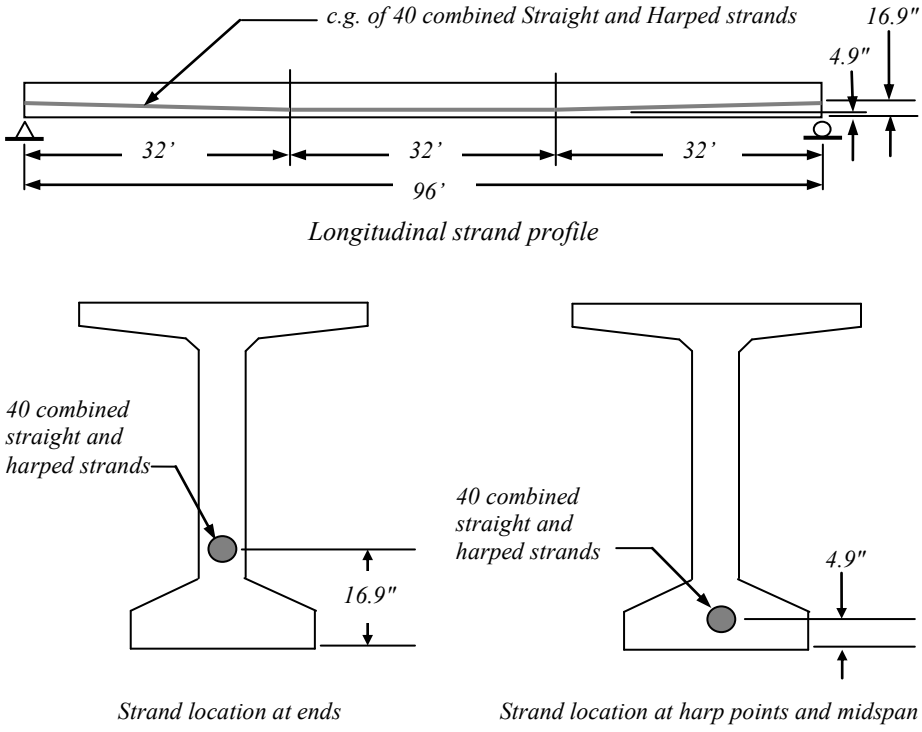

Figure 8. Longitudinal strand profile and locations of the centroid of combined straight and harped strands

5.3 Compute prestress loss due to the elastic shortening of the girder

For the first iteration, assuming that the prestressing force in tendons immediately after prestress loss due to the elastic shortening of concrete is 90 percent of the initial prestressing force before prestress transfer, that is:

$$f_{pbt} - \Delta f_{pES} = 0.9 f_{pbt} = 0.9(0.75) f_{pu} = 0.9(0.75)(270\text{ksi}) = 182.25 \text{ ksi}$$

From Eq. (5), one has:

$$P_i = A_{ps}(f_{pbt} - \Delta f_{pES}) = (6.12 \text{ in.}^2)(182.25 \text{ ksi}) = 1115.37 \text{ kips}$$

Since A_g = 659 ft^2 (referring to Table 1) and L = 96 ft, the moment at the midspan due to the weight of the girder (the weight of the girder is estimated to be 0.15 kips/ft^3) at the time of prestressing can be computed to be:

$$M_g = \frac{wL^2}{8} = \frac{(0.15\text{kips/ft}^3)(659/144)\text{ft}^2(96\text{ft})^2(12\text{in./ft})}{8} = 9489.6 \text{ kip-in.}$$

Note that, in the above equation, "w" is the self-weight per unit length of the girder. Also, referring to *Fig. 6*, the distance between the centroid of the gross concrete section and the bottom fiber of the girder can be computed to be:

$$Y_b = 54 \text{ in.} - \bar{y} = 54 \text{ in.} - 26.366 \text{ in.} = 27.634 \text{ in.}$$

Furthermore, referring to *Fig.* 8, the average prestressed steel eccentricity at the midspan thus can be computed to be:

$$e_m = 27.634 \text{ in.} - 4.9 \text{ in.} = 22.734 \text{ in.}$$

From Eq. (4), one has:

$$\begin{aligned} f_{cgp} &= -\frac{P_i}{A_g} - \frac{(P_i e_m)e_m}{I_g} + \frac{M_g e_m}{I_g} \\ &= -\frac{1115.37}{659} - \frac{(1115.37)(22.734)^2}{268{,}051} + \frac{9489.6(22.734)}{268{,}051} \\ &= (-)3.038 \text{ ksi} \end{aligned}$$

From Eq. (3), one has:

$$\Delta f_{pES} = \frac{E_p}{E_{ci}} f_{cgp} = \frac{28{,}500}{4458}(3.038) = 19.42 \text{ ksi}$$

For the second iteration, one has:

$$P_i = A_{ps}(f_{pbt} - \Delta f_{pES}) = (6.12 \text{ in.}^2)[0.75(270 \text{ ksi}) - 19.42 \text{ ksi}] = 1120.45 \text{ kips}$$

From Eq. (4), one has:

$$f_{cgp} = -\frac{1120.45}{659} - \frac{(1120.45)(22.734)^2}{268{,}051} + \frac{9489.6(22.734)}{268{,}051} = (-)3.056 \text{ ksi}$$

From Eq. (3), one has:

$$\Delta f_{pES} = \frac{E_p}{E_{ci}} f_{cgp} = \frac{28{,}500}{4458}(3.056) = 19.54 \text{ ksi}$$

For the third iteration, one has:

$$P_i = A_{ps}(f_{pbt} - \Delta f_{pES}) = (6.12 \text{ in.}^2)[0.75(270 \text{ ksi}) - 19.54 \text{ ksi}] = 1119.72 \text{ kips}$$

From Eq. (4), one has:

$$f_{cgp} = -\frac{1120.45}{659} - \frac{(1119.72)(22.734)^2}{268{,}051} + \frac{9489.6(22.734)}{268{,}051} = (-)3.054 \text{ ksi}$$

From Eq. (3), one has:

$$\Delta f_{pES} = \frac{E_p}{E_{ci}} f_{cgp} = \frac{28{,}500}{4458}(3.054) = 19.52 \text{ ksi}$$

For the fourth iteration, one has:

$$P_i = A_{ps}(f_{pbt} - \Delta f_{pES}) = (6.12 \text{ in.}^2)[0.75(270 \text{ ksi}) - 19.52 \text{ ksi}] = 1119.84 \text{ kips}$$

From Eq. (4), one has:

$$f_{cgp} = -\frac{1120.45}{659} - \frac{(1119.84)(22.734)^2}{268{,}051} + \frac{9489.6(22.734)}{268{,}051} = (-)3.054 \text{ ksi}$$

From Eq. (3), one has:

$$\Delta f_{pES} = \frac{E_p}{E_{ci}} f_{cgp} = \frac{28{,}500}{4458}(3.054) = 19.52 \text{ ksi}$$

Since the prestress loss at the midspan due to the elastic shortening of the girder determined from the fourth iteration is the same as that determined from the third iteration, the accuracy of the result ($\Delta f_{pES} = 19.52$ ksi) is acceptable.

Alternatively, to avoid multiple iterations, Δf_{pES} can be directly determined using Eq. (6):

$$\Delta f_{pES} = \frac{A_{ps} f_{pbt} (I_g + e_m^2 A_g) - e_m M_g A_g}{A_{ps}(I_g + e_m^2 A_g) + \frac{A_g I_g E_{ci}}{E_p}}$$

$$= \frac{6.12(202.5)[268051 + (22.734)^2(659)] - 22.734(9489.6)(659)}{6.12[268051 + (22.734)^2(659)] + \frac{659(268051)(4458)}{28500}}$$

$$= 19.52 \text{ ksi}$$

The prestressing force in the prestressed steel at the midspan immediately after prestress loss due to the elastic shortening of concrete thus can be computed to be:

$$P_i = A_{ps}(f_{pbt} - \Delta f_{pES}) = (6.12 \text{ in.}^2)[0.75(270 \text{ ksi}) - 19.52 \text{ ksi}] = 1119.84 \text{ kips}$$

Follow the calculation procedure demonstrated above, the initial prestressing forces, P_i, along the pretensioned girder shown in *Fig. 8* are computed and are shown in Table 2 and *Fig. 9*.

Table 2. The initial prestressing forces acting along the pretensioned girder

x (the distance of the section measured from the left support shown in *Fig. 9*) (ft)	e (the vertical distance between c.g.s. and c.g.c.) (in.)	M_g (the moment due to the weight of the girder) (kip-in.)	Δf_{pES} (prestress loss due to the elastic shortening of the girder) (ksi)	P_i (the initial prestressing forces) (kips)
0	10.734	0	14.34	1151.57
4	12.234	1515.7	14.80	1148.71
8	13.734	2899.6	15.32	1145.56
12	15.234	4151.7	15.89	1142.04
16	16.734	5272.0	16.54	1138.09
20	18.234	6260.5	17.26	1133.64
24	19.734	7117.2	18.08	1128.64
28	21.234	7842.1	19.00	1123.02
32	22.734	8435.2	20.03	1116.74
36	22.734	8896.5	19.81	1118.09
40	22.734	9226.0	19.65	1119.06
44	22.734	9423.7	19.55	1119.63
48	22.734	9489.6	19.52	1119.84

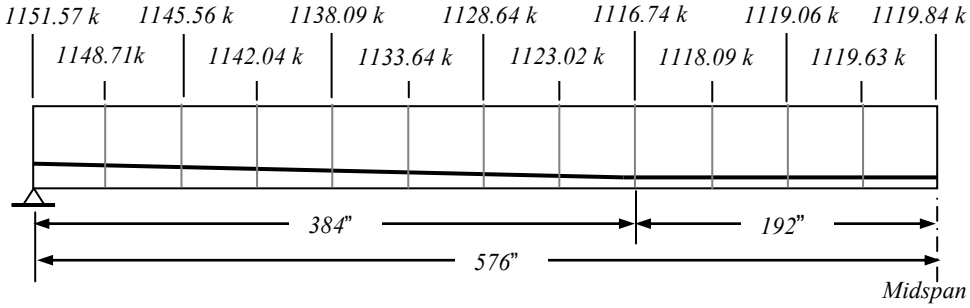

Figure 9. Various prestressing forces acting along the girder immediately after prestress loss due to the elastic shortening of concrete

As shown in *Fig. 9,* since the magnitude of the variation of the initial prestressing forces acting along the tendons is not significant (about 3% in this example), the inconstant prestressing forces acting along the girder have no significant effect on the deflection of the girder.

5.4 Compute the camber of the girder immediately after prestress loss due to the elastic shortening of the girder

Five different approaches for the computation of the camber of the girder immediately after prestress loss due to the elastic shortening of the girder are presented in this paper: (I) the equivalent load method using the traditional hand-calculated approach and gross section properties neglecting prestressed steel, (II) the equivalent load method using the finite element analysis approach and gross section properties neglecting prestressed steel, (III) the combined equivalent load and P-δ effect method using gross section properties neglecting prestressed steel and the finite element analysis approach accounting for geometric nonlinearity, (IV) the equivalent load method using the finite element analysis approach and section properties accounting for prestressed steel, and (V) the thermal effects method using the finite element analysis approach and section properties accounting for prestressed steel.

(I) The equivalent load method using the traditional hand-calculated approach and gross section properties neglecting prestressed steel:
Referring to *Figs. 2, 6, & 7*, one has e = 54 – 26.366 – 4 = 23.634 in. and $P_s = P_i$ = 1119.84(28/40) = 783.89 kips. The midspan camber due to prestressing of the straight strands thus can be computed using Eq. (1):

$$\Delta = \frac{(96\times 12)^2}{8(4458)(268051)}(783.89\times 23.634) = 2.572 \text{ in. } \uparrow \text{ (upward)}$$

Furthermore, referring to *Figs. 3, 6, & 7*, one has $e_1 = 47 - 7 = 40$ in., $e_2 = (54 - 26.366) - 47 = (-)19.366$ in., $a = 384$ in. and $P_s = P_i = 1119.84(12/40) = 335.95$ kips. The midspan camber due to prestressing of the harped strands thus can be computed using Eq. (2):

$$\Delta = \frac{335.95(40)}{24(4458)(268051)}[3(1152)^2 - 4(384)^2] + \frac{(1152)^2}{8(4458)(268051)}(335.95)(-19.366)$$

$$= 1.589 - 0.903 = 0.686 \text{ in.} \uparrow \text{(upward)}$$

The total midspan camber due to prestressing of the straight and the harped strands thus is:

$$\Delta = 2.572 + 0.686 = 3.258 \text{ in.} \uparrow \text{(upward)}$$

The above computation procedure can be abbreviated using the combined straight and harped strands profile, as shown in *Fig. 8*. Referring to *Figs. 3, 6, & 8*, one has $e_1 = 16.9 - 4.9 = 12$ in., $e_2 = (54 - 26.366) - 16.9 = 10.734$ in., $a = 384$ in., and $P_s = P_i = 1119.84$ kips. The midspan camber due to prestressing of the combined straight and harped strands thus can be computed using Eq. (2):

$$\Delta = \frac{(1119.84)(12)}{24(4458)(268051)}[3(1152)^2 - 4(384)^2] + \frac{(1152)^2}{8(4458)(268051)}(1119.84)(10.734)$$

$$= 1.589 + 1.669 = 3.258 \text{ in.} \uparrow \text{(upward)}$$

The midspan deflection due to the self-weight of the girder can be computed using Eq. (9) [6]:

$$\Delta = \frac{5}{384}\left(\frac{wL^4}{EI}\right) \tag{9}$$

where: w is the self-weight per unit length of the girder.

The self-weight per unit length of the girder can be computed to be $w = (0.15 \text{ kips/ft}^3)\,[(659/144)\text{ ft}^3] = 0.6864$ kips/ft. From Eq. (9), one has:

$$\Delta = \frac{5}{384}\left[\frac{(0.6864)(96)^4(12)^3}{(4458)(268051)}\right] = 1.098 \text{ in.} \downarrow \text{(downward)}$$

Therefore, the net midspan camber (upward deflection) can be computed to be:

$$\Delta = 3.258 - 1.098 = 2.160 \text{ in.} \uparrow \text{(upward)}$$

(II) The equivalent load method using the finite element analysis approach and gross section properties neglecting prestressed steel:
Referring to *Figs. 3(a)* & *8*, one has tan $\theta = (16.9\text{-}4.9)/(32\times12)$; from which, $\theta = 1.7899^{o}$. Therefore, $P_i \cos\theta = 1119.84$ kips $\times \cos 1.7899^{o} = 1119.29$ kips and $P_i \sin\theta = 1119.84$ kips $\times \sin 1.7899^{o} = 34.98$ kips. The equivalent loads (produced by the pretensioned steel) and the loaded locations are shown in *Fig. 10(a)*. The self-weight of the girder is shown in *Fig. 10(b)*. Note that the c.g.c line is the assumed location at which the self-weight of the girder is applied.

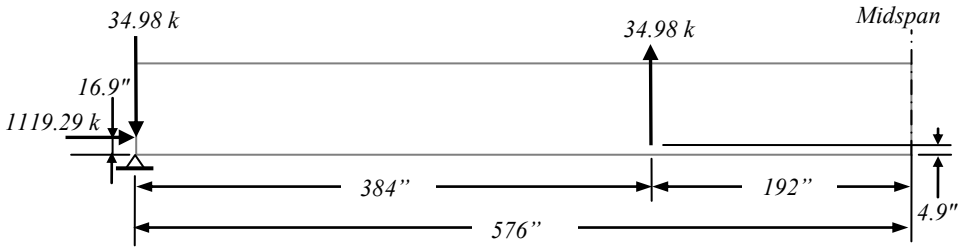

(a) Equivalent loads produced by the pretensioned steel

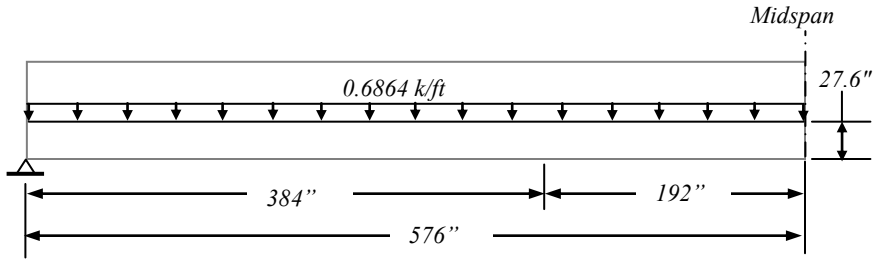

(b) Self-weight of the girder

Figure 10. Equivalent loads (produced by pretensioned steel) and the self-weight of the girder

Based on *Fig. 10*, a computer model composed of numerous 3-D solid elements for the girder cross section was constructed (shown in *Fig. 11*) for the finite element analysis using the NISA/DISPLAY software [10]. Note that the cross section of the girder shown in *Fig. 11* incorporates the elevations of 16.9 in. (the elevation to be loaded by the equivalent load produced by the prestressed steel at the end of the girder), 4.9 in. (the elevation to be loaded by the equivalent load produced by the prestressed steel at the harp point of the c.g.s. line), and 27.6 in. (the elevation of the c.g.c. line of the girder to be loaded by the self-weight of the girder).

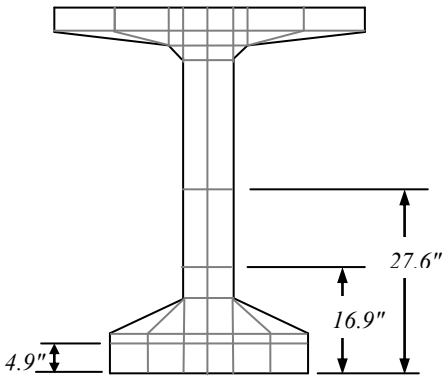

Figure 11. Computer model of the cross section of the girder neglecting prestressed steel

From the finite element analysis using the equivalent loads produced by the pretensioned steel shown in *Fig. 10(a)*, the camber at the midspan of the girder due to the prestressing force immediately after prestress transfer was found to be 3.272 in., as shown in *Fig. 12*. Also, from the finite element analysis using the load shown in *Fig. 10(b),* the downward deflection at the midspan of the girder due to the self-weight of the girder was found to be 1.116 in., as shown in *Fig. 13*.

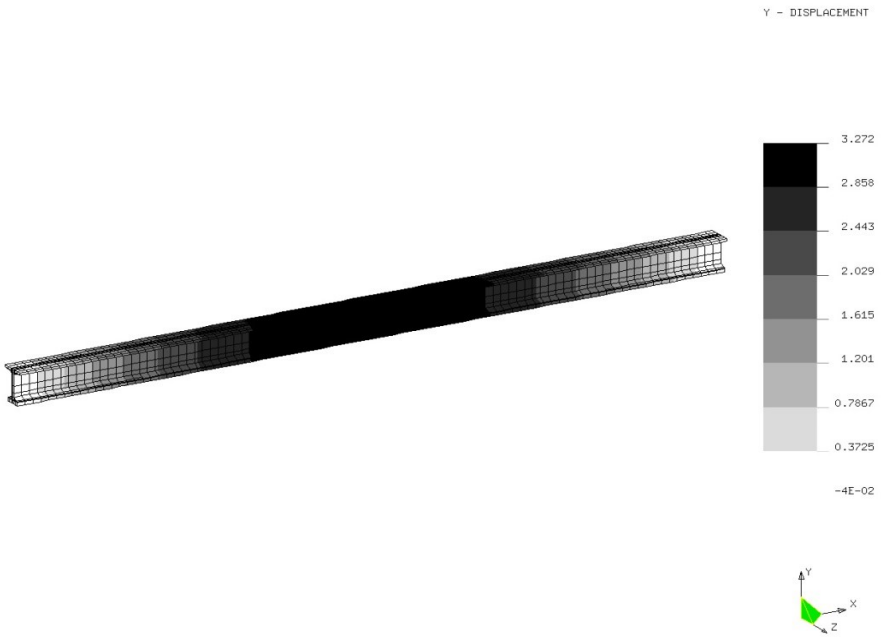

Figure 12. Camber due to the prestressing force immediately after prestress transfer, computed using first-order elastic finite element analysis

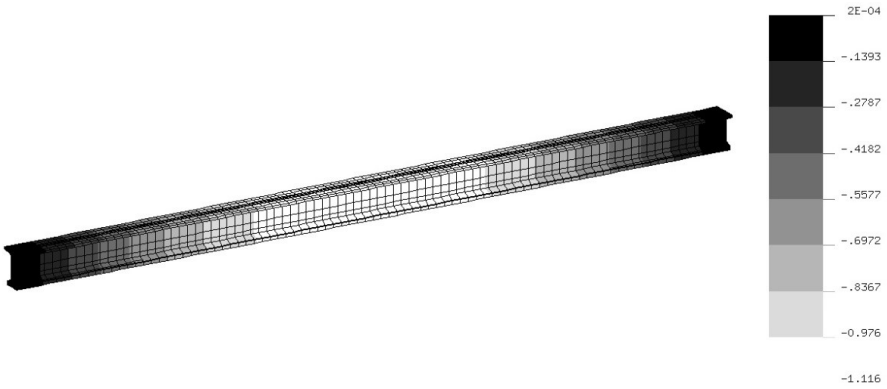

Figure 13. Downward deflection due to the self-weight of the girder, computed using first-order elastic finite element analysis

From *Figs. 12 & 13*, the net midspan camber can be computed to be:

$$\Delta = 3.272 - 1.116 = 2.156 \text{ in.} \uparrow \text{(upward)}$$

Alternatively, the camber at the midspan of the girder due to the combined equivalent loads (produced by the pretensioned steel) and the self-weight of the girder shown in *Fig. 14* was found to be 2.155 in. (≈ 2.156 in. as computed above), as shown in *Fig. 15*.

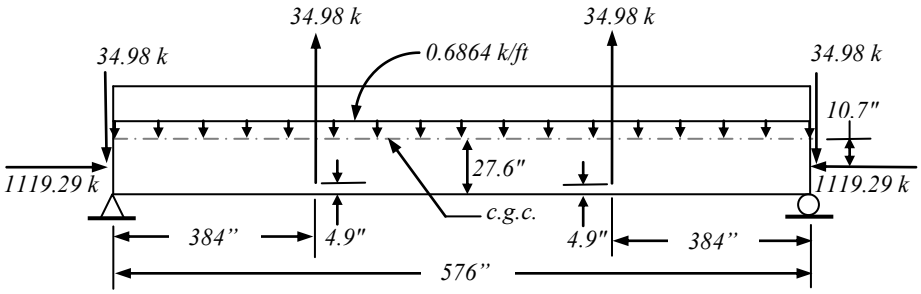

Figure 14. Equivalent loads (produced by pretensioned steel) in combination with the self-weight of the girder

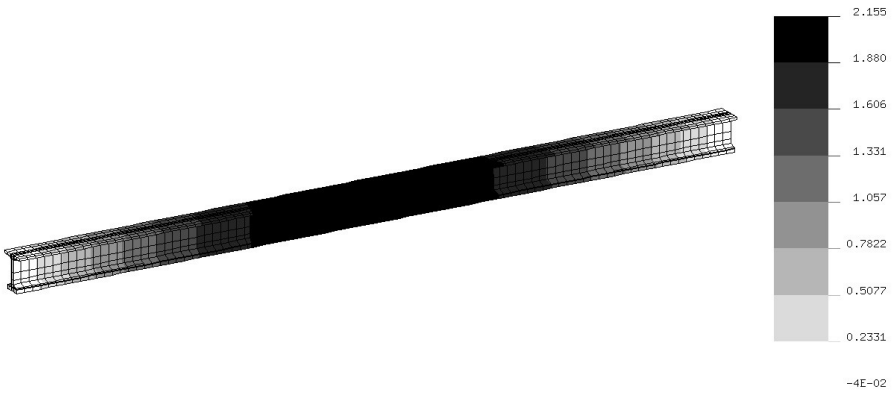

Figure 15. Camber due to equivalent loads (produced by pretensioned steel) in combination with the self-weight of the girder, computed using first-order elastic finite element analysis

(III) The combined equivalent load and P-δ effect method using gross section properties neglecting prestressed steel and the finite element analysis approach accounting for geometric nonlinearity:
Referring to *Fig. 16*, the deflection δ at the midspan of the structural element causes additional deflection $y_{p-\delta}$ due to the axial force (P) acting at the position that has been displaced by an amount δ. This is the so-called P-δ effect, that is, the additional deflection $y_{p-\delta}$ at the midspan of the element is the portion of the deflection caused by the secondary bending moment due to the P-δ effect.

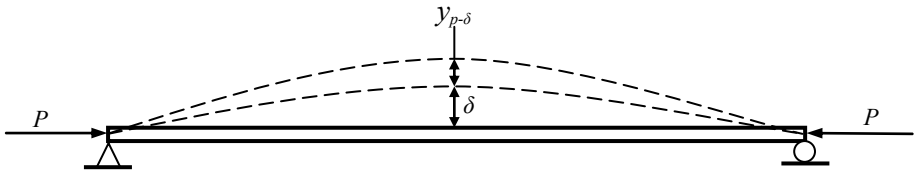

Figure 16. P-δ effect on the deflection of a structural element subject to an axial force

From the Camber Computation Approach (II), the camber δ (shown in *Fig. 16*) was found be to be 2.155 in. for this girder (shown in *Fig. 15*) using the first-order elastic finite element analysis. Since the additional deflection $y_{p-\delta}$ at the midspan of the girder can only be determined using the second-order elastic analysis, a nonlinear static finite element analysis accounting for geometric nonlinearity was conducted in order to carry out the second-order elastic analysis. A pseudo time of 100 has been used for the time span, which is equivalent to load increments or steps (from zero to that shown in *Fig. 14*) for the geometric

nonlinear static finite element analysis. The final camber (at the time step = 100) of the girder due to the self-weight of the girder and the prestressing force immediately after prestress transfer using the finite element analysis accounting for geometric nonlinearity (P-δ effect) was found to be 2.462 in., as shown in *Fig. 17*. Therefore, the additional deflection $y_{p-\delta}$ at the midspan of the girder, as shown in *Fig. 16*, due to P-δ effect can be computed to be:

$$y_{p-\delta} = 2.462 - 2.155 = 0.307 \text{ in.} \uparrow \text{(upward)}$$

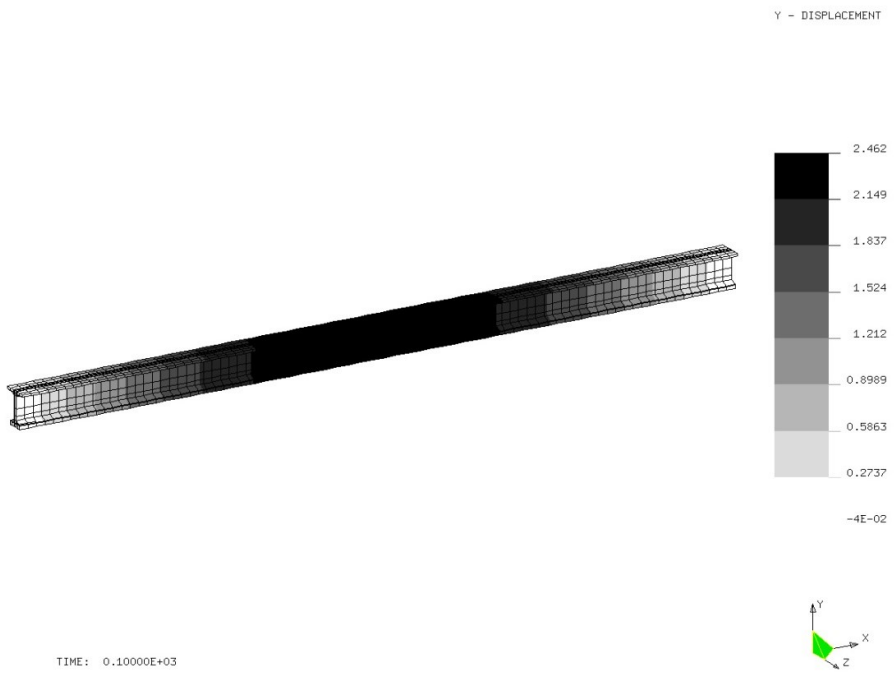

Figure 17. Camber due to equivalent loads (produced by pretensioned steel) in combination with the self-weight of the girder, computed using the finite element analysis accounting for geometric nonlinearity (P-δ effect)

(IV) The equivalent load method using the finite element analysis approach and section properties accounting for prestressed steel:
Based on the longitudinal strand profile, a computer model composed of numerous 3-D solid elements for the girder cross section was constructed, as shown in *Fig. 18*, for the finite element analysis. Note that the cross section of the girder shown in *Fig. 18* incorporates the elevations of 16.9 in. (the elevation to be loaded by the equivalent load produced by the prestressed steel at the end of the girder), 4.9 in. (the elevation to be loaded by the equivalent load produced by

the prestressed steel at the harp point of the c.g.s. line), and 27.6 in. (the elevation of the c.g.c. line of the girder to be loaded by the self-weight of the girder).

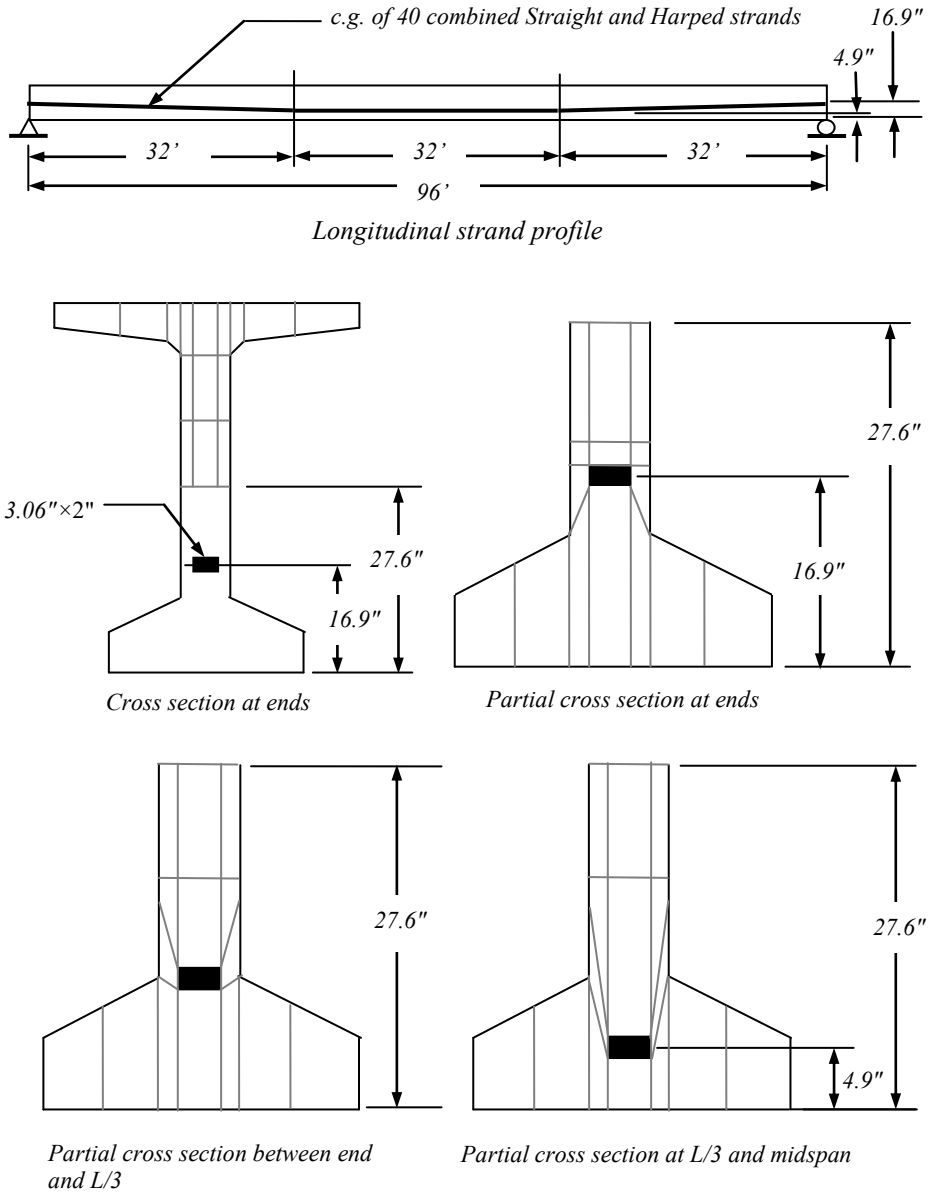

Figure 18. Computer model of the girder cross section accounting for prestressed steel

From the finite element analysis using equivalent loads produced by the pretensioned steel shown in *Fig. 10(a)*, the camber at the midspan of the girder due to the prestressing force immediately after transfer was found to be 2.945 in., as shown in *Fig. 19*. Also, from the finite element analysis using the load shown in *Fig. 10(b),* the downward deflection at the midspan of the girder due to the self-weight of the girder was found to be 1.051 in., as shown in *Fig. 20*. From *Figs. 19 & 20*, the net midspan camber can be computed to be:

$$\Delta = 2.945 - 1.051 = 1.894 \text{ in.} \uparrow \text{(upward)}$$

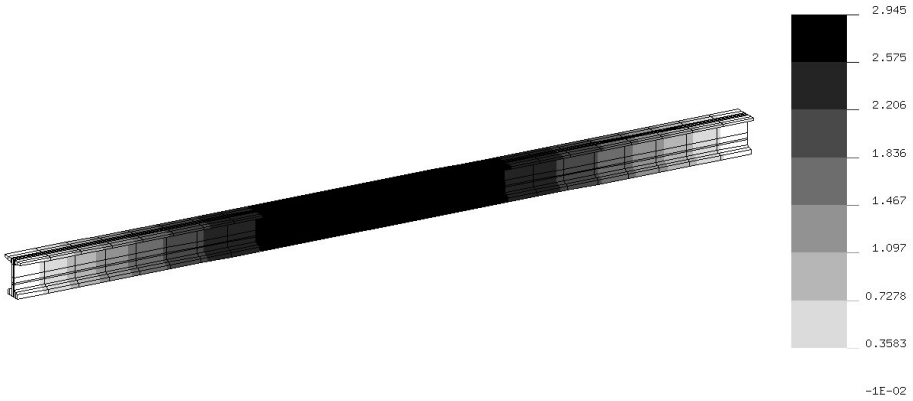

Figure 19. Camber of the girder (with its cross section property accounting for prestressed steel) due to the prestressing force immediately after prestress transfer

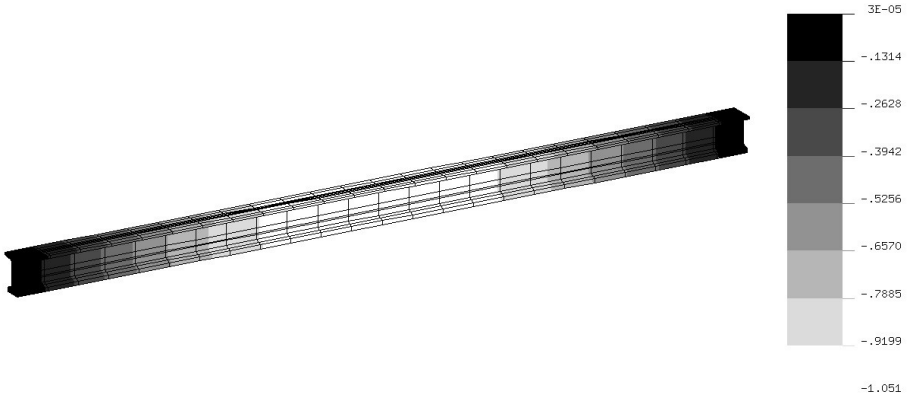

Figure 20. Downward deflection of the girder (with its cross section property accounting for prestressed steel) due to the self-weight of the girder

(V) The thermal effects method using the finite element analysis approach and section properties accounting for prestressed steel:
The theory of "thermal effects on steel" is utilized in this approach to simulate prestressing forces in tendons. Since the change in unit stress in prestressed steel is the product of "ε" and "Δt" (where ε is the thermal expansion coefficient of prestressed steel and Δt is the change in temperature of prestressed steel), the expected prestressing force (P_i = 1119.84 kips) can be simulated using a random thermal expansion coefficient of prestressed steel ($\varepsilon = 6.5\times10^{-6}$ 1/°F) multiplied by a corresponding temperature change of prestressed steel (Δt = 987.75 °F). Therefore, from Eq. (8), one has: P_i = 1119.84 kips = $A_{ps}E_p\varepsilon(\Delta t)$ = (6.12 in^2)(28500 ksi)(6.5×10^{-6} 1/°F)(987.75 °F). A finite element analysis was carried out using the thermal effects method and the camber of the girder due to the thermal effect on the simulated prestressing force is shown in *Fig. 21*.

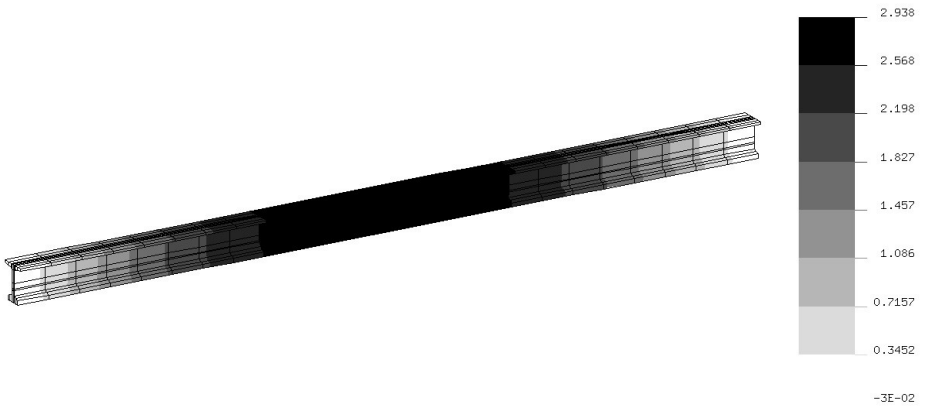

Figure 21. Camber of the girder (with its cross section property accounting for prestressed steel) computed using the thermal effects method

5.5 Summary of the results

The deflections at the midspan of the girder due to the prestressing force immediately after prestress transfer and the self-weight of the girder computed using various approaches (Approaches I through V) are summarized in Table 3.

Table 3. The deflection at the midspan of the girder due to the prestressing force immediately after transfer and the self-weight of the girder

approach	deflection due to prestressing force	deflection due to self-weight	final deflection
I	3.258 in. ↑	1.098 in. ↓	2.160 in. ↑
II	3.272 in. ↑	1.116 in. ↓	2.156 in. ↑
III	not applicable	not applicable	2.462 in. ↑
IV	2.945 in. ↑	1.051 in. ↓	1.894 in. ↑
V	2.938 in. ↑	1.051 in. ↓	1.887 in. ↑

As shown in Table 3, Approach II can be used to validate the results obtained from Approach I; also, Approach V can be used to validate the results obtained from Approach IV.

6 CONCLUSIONS

Five different approaches for the computation of the camber in a pretensioned girder immediately after prestress loss due to the elastic shortening of the girder are presented in this paper. Approaches (I) and (II) used the equivalent load method and gross section properties neglecting prestressed steel. Approach (III) used the combined equivalent load and P-δ effect method and gross section properties neglecting prestressed steel. Approaches (IV) and (V) used the equivalent load method and the thermal effects method, respectively, while section properties of both approaches accounted for the use of prestressed steel. Approach (I), which uses the gross section properties and neglects prestressed steel as well as the P-δ effect due to axial prestressing forces, is a conventionally used approach for the computation of deflections in simply supported pretentioned concrete girders. This study concludes that (1) the deflections considerably increased (by about 14 % in the example demonstrated in this study) if the P-δ effect is considered, and (2) the deflections considerably decreased (by about 13 % in the example demonstrated in this study) if the section properties accounting for prestressed steel is considered. In addition, this study also concludes that since the magnitude of the variation of the prestressing forces acting along the tendons is not significant, the inconstant prestressing forces acting along the girder have limited effects on the deflection of the girder. Therefore, for the computation of cambers of a simply supported girder, the magnitude of the prestressing force acting at locations other than the midspan of the girder can be treated as the same as that at the midspan.

REFERENCES

[1] California Department of Transportation, *Bridge Design Practice*, 4th Edition, California Department of Transportation, 2015.

[2] Hueste, MBD, Adil, MSU, Adnan, M, Keating, PB, *Impact of LRFD Specifications on Design of Texas Bridges Volume 2: Prestressed Concrete Bridge Girder Design Examples*, Texas Transportation Institute, 2006.

[3] Wisconsin Department of Transportation, *Bridge Manual*, Wisconsin Department of Transportation, 2015.

[4] Lin, TY, *Design of Prestressed Concrete Structures*, 2nd Ed., John Wiley & Sons, Inc., New York, 1963.

[5] Nawy, EG, *Prestressed Concrete: A Fundamental Approach*, 5th Ed., Pearson Education, Inc., Upper Saddle River, New Jersey, 2010.

[6] Timoshenko, S, Young, DH, *Elements of Strength of Materials*, 5th Ed., D. Van Nostrand Company, Inc., Princeton, New Jersey, 1968.

[7] American Concrete Institute, *Building Code Requirements for Structural Concrete (ACI 318-11) and Commentary,* American Concrete Institute, Farmington Hills, MI, 2011.

[8] American Association of State Highway and Transportation Officials, *AASHTO LRFD Bridge Design Specifications,* American Association of State Highway and Transportation Officials, Washington, DC, 2012.
[9] Spiegel, L, Limbrunner, GF, A*pplied Statics and Strength of Materials*, 3rd Ed., Prentice-Hall, Inc., Upper Saddle River, New Jersey, 1999.
[10] NISA, *NISA User's Manual*, the Cranes Software, Inc., Troy, MI, 2005.